BIOMIMETIC SYNTHESIS OF GUIDED-TISSUE REGENERATION HYDROXYAPATITE/POLYVINL ALCOHOL NANOCOMPOSITE SCAFFOLDS: INFLUENCE OF ALIGNATE ON MECHANICAL AND BIOLOGICAL PROPERTIES.

E. TOLBA[1], B. M. ABD-ELHADY[1], B. ELKHOLY[1], H.ELKADY[2],M. ELTONSI[3]

[1.] Biomaterial Department, National Research Center, Cairo, Egypt.
[2.] Civil Engineering Department, National Research Center, Cairo, Egypt.
[3.] Physics Department, Faculty of science, El-Mansoura University, El-Mansoura, Egypt
hala.elkady@gmail.com

Abstract: This paper presents a part of a major research, in which HA/PVA/alginate scaffolds -with different alginate compositions -up to 20wt% were fabricated by a modified freeze-extraction method. This method includes the physical cross-linking of PVA and chemical cross-linking of the alginate. Characterization of the prepared scaffolds was performed by morphology observations using scanning electron microscopy (SEM). Different physical properties – as porosity and density-were measured. It was noticed that by increasing alginate composition scaffolds exhibited highly porous, open-cellular pore structures with almost porosity about 90%, regardless of alginate composition and the pore sizes from about 150 to about 300μm.The In Vitro bioactivity and biodegradability of nano-composite scaffolds were investigated by incubation in simulated body fluid (SBF) and water under osteoclastic resorption conditions, respectively. The in-vitro bioactivity test indicating the higher bone-bonding ability of the biomimetically synthesized a scaffold that is awarded by the fast formation of bonelike apatite on their surfaces within one day. Also The addition of alginate to HA/PVA scaffolds increased the biodegradability compared with that one without alginate. Mechanical behavior of scaffolds was investigated under axial loading. Scaffolds stress strain behavior, maximum true stress, and elastic moduli, were calculated. It was found that increasing alginate content from 0 to 20% by weight, decreased the compressive modulus from 85.3 to 44.7 MPa, whereas the maximum compressive strength decreased from 6 to 5 MPa. Finally, it was concluded that the proposed scaffolds expressed promising performance, despite of the resulting degradation in their mechanical behavior. The obtained compressive strength and modulus of elasticity were still within satisfactory limits. [Journal of American Science 2010;6(7):239-249]. (ISSN: 1545-1003).

Keywords: Tissue re-generation, Poly(vinyl), composites, scaffolds

1. Introduction

One of the main goals in bone tissue engineering is to develop biodegradable materials as bone graft substitutes, especially for filling large defects [1-3]. Besides bone forming cells and growth factors, synthetic biomaterials served as scaffolds play a critical role in bone tissue engineering and osteogenesis. They provide a three dimensional (3-D) space for cell growth and extracellular matrix (ECM) formation, and structural support for the newly formed bone tissue. The ideal synthetic scaffolds for osteogenesis should meet certain criteria to serve this function, including good biocompatibility, sufficient mechanical properties, and adequate biodegradability at a controlled rate commensurate with remodeling [4, 5]. Being the major mineral component of natural bone and structurally similar to the bone, hydroxyapatite (HA) is the prospective one of inorganic biomaterials for bone regeneration[6,7]. HA ceramics were high biocompatible in bone tissue and had a high osteogenic potential (osteo-conduction and osteo-integration), but the brittleness and fatigue failure in the body limit their clinical applications only for unloading bearing repair and substitute [8, 9]. This fact restricts the use of these materials in a wide range of applications. One alternative that is being considered and studied is the production of composites and hybrid systems. Hence, the development of composite materials is regarded as a promising approach for preparing bioactive scaffolds [10]. Composites, which include synthetic and biological polymers with HA, have the potential capability of combining bioactive behavior with adequate mechanical properties.

Among several choices of polymers, poly(vinyl alcohol) (PVA), a water-soluble polyhydroxy

polymer, has been frequently explored as an implant material in biomedical applications such as drug delivery systems, dialysis membranes, wound dressing, artificial skin, cardiovascular devices and surgical repairs because of its excellent mechanical strength, biocompatibility and non-toxicity [11,12]. PVA is considered as a biologically friendly material but with some reduced integration to living tissues due to its relative limited biodegradability and bioactivity, compared to poly(ethylene oxide) (PEO), poly(lactic-co-glycolic acid) (PLGA) and others. Therefore, it is promising to blend PVA with biopolymers such as alginate to produce a new polymeric system applicable for a variety of purposes [13]. In order to overcome the limited biological performance of synthetic polymers and to enhance the mechanical characteristics of biopolymers, a new class of specially designed materials, 'bioartificial polymeric materials', has been introduced [14]. These materials based on blends of both synthetic and natural polymers such as alginate could be usefully employed as biomaterials. Alginate, a polysaccharide derived from brown seaweed, has been widely utilized as cell carriers since the 1970s [15] due to the simplicity for fabricating cell-immobilized beads or 3D porous scaffolds, low price compared to proteins or other natural polymers and non-toxicity to cells. It is also approved by the Food and Drug Administration (FDA) for human use as wound dressing material and food additive. The alginate, the monovalent salt form of alginic acid is a linear block copolymer composed of *β*-D-mannuronate (M-block) and *α*-L-guluronate (G-block) linked by 1,4-glycoside linkage [16]. The G-block of alginate has correspondingly high affinities for divalent ions such as calcium (Ca2+), strontium (Sr2+) and barium (Ba2+) at room temperature and thus in an aqueous solution of divalent ions, the alginate chains are rapidly cross-linked *via* the stacking of G-blocks to form an egg-box structure and subsequently become gel [17].

In our previous work, HA/PVA nanocomposite was synthesized by using biomimetic method and subject to freeze extraction technique in conjugation with liquid descant drying regime to obtain the three dimensional HA/PVA scaffolds[18]. The resultant scaffolds exhibit a high interconnectivity and maximum pore size of 150 µm, indicating preferred morphology for tissue engineering application.

In the presented study, a series of HA/PVA/Alginate scaffolds with 0, 5, 10 and 20% alginate were fabricated by freeze extraction method followed by chemical cross-linking of alginate. The porosity, pore size, mechanical property of the scaffolds was investigated as functions of alginate content. In addition, the in vitro bioactivity and biodegradability of nano-composite scaffolds were investigated by incubation in simulated body fluid (SBF) and water under osteoclastic resorption conditions, respectively. The emphasis of this study was placed on the development of a novel scaffold suitable for hepatic tissue-engineering application.

Mechanical properties of a scaffold are important both for integrity during handling and implantation, and for support of tissue subject to load during healing. Measures to improve mechanical properties without sacrificing other properties (biocompatibility, osteoconductivity) are thus highly desirable. There are numerous reports in literature describing the improvement of the mechanical properties of polymers by adding bioactive inorganic materials, such as hydroxyapatite (HA). As with the modulus, it is natural for the strength of the scaffold to increase with increasing volume fraction of the filler content, especially if there is strong interaction between the matrix and the filler. A careful literature survey has shown that polymer/HA composites are complex systems [27-29].

2. Experimental procedure for scaffolds manufacturing.

2.1. Materials

Through out the entire preparation part of the work, double distilled water as well as the following reagent-grade chemicals were used calcium hydroxide [$Ca(OH)_2$],BDH-Laboratory,England; ammonium dihydrogen phosphate($NH_4H_2PO_4$), MERCK, Germany; PVA with an average molecular weight of 124,000 and degree of hydrolysis 98 - 99%, Loba Chemie, India. Sodium alginate (also called algin or alginic acid sodium salt) from Sigma (USA). Ammonia solution (NH_4OH) (33%), absolute Ethanol and pure Acetone, El Nasr Pharmaceuticals and Chemicals Co. Egypt.

2.2. Samples preparation

2.2.1. Synthesis of HA/PVA/ alginate gels

HA/PVA/alginate gels with different alginate compositions (0, 5, 10, and 20 wt %) were fabricated by using the freeze extraction method. Making a deviation from our early employed post precipitation technique, including freeze extraction method (18), the present study involves chemical cross-linking of alginate extracted gels. In brief, Sodium alginate was easily soluble in cold water. Then, the solution was added to the synthesized HA/PVA mix solution. The mixture was then left under stirring for approximately 4 h at room temperature until a completely homogenous solution was obtained. After each the mixture solutions were poured in cylindrical Teflon vials. The freeze extraction step was used necessary to obtain the

physically coherent gels having the ability to keep their original shape (mold shape) before alginate cross-linking. The obtained gels were then immersed in 5 wt% $CaCl_2$ solution for 12 h to chemical cross-linking of alginate with calcium ions. The resultant gels with 0, 5, 10 and 20% alginate were designated by the abbreviations AHP, 5AHPG, 10AHPG and 20AHPG, respectively.

3. Samples characterization

3.1. Bulk density and apparent porosity measurement

The bulk density and apparent porosity of the porous scaffolds were measured by using the Archimedes' principle [19]. This method is based on soaking the samples under kerosene for 2hrs in a vacuum desiccator to saturate their open-pore structure with the latter. The weight of saturated sample suspended in kerosene (Wi) and its saturated weight in air after removal of kerosene film from outer surface (Ws) were recorded. Triplicate measurements were carried out to obtain their mean values. Bulk density (D) and apparent porosity (P) were calculated according to the following equations (1):

$$D=\frac{W}{(Ws-Wi)}x\rho$$

$$P=\frac{(Ws-W)}{(Ws-Wi)}x100\% \qquad (1)$$

ρ= specific gravity of kerosene (0.78).

3.2. Morphological observations

Morphological observation of the resultant scaffolds was preformed by Philips XL 30 Scanning Electron Microscope (SEM) with an acceleration voltage of 30 kV. Whereby specimens were cut from liquid nitrogen-treated (frozen) scaffold to avoid disturbing of the pore structure. Specimens were placed on a stub using a carbon sticker and were examined under the microscope after the samples were sputtered with a thin coat of gold.

3.3- Axial Compression Mechanical test

3.3.1-Instrumentation and test setup

A universal (SHUMADZU) testing machine was utilized to conduct the compression mechanical test. A computer-controlled module monitored and controlled the entire testing. Input and output data were recorded related to compression test using the machine acquisition system. Three specimens were cast for each of the investigated scaffolds: $AHP_{10\text{-}6}$, and $20AHPG_{10\text{-}6.}$ Dimensions of each sample were measured prior to testing. Averages of measured dimensions are 16 and 14 mm (diameter and height respectively.) Tests were conducted in room temperature. The crosshead speed was set at 0.5 mm/min.

3.4 (In-Vitro Test):

3.4.1- Water-binding capacity testing

The dry scaffolds ($AHP_{10\text{-}6}$, $5AHPG_{10\text{-}6}$, $10AHPG_{10\text{-}6}$ and $20AHPG_{10\text{-}6}$) were immersed were placed in a small bottle containing 20 ml water (pH 7.4) and incubated at 37°C for 24h. The water binding capacity (expressed as a percentage) was calculated by comparing the initial weight (W_0) with the wet weight after swelling (W_1), as shown in Equation (2). Three individual experiments were performed, and then the average value was gained.

$$\text{Water - binding capacity} = \frac{W1-Wo}{Wo}x100 \qquad (2)$$

3.4.2- Biodegradation testing

The in-vitro biodegradation study of the resultant scaffolds ($AHP_{10\text{-}6}$, $5AHPG_{10\text{-}6}$, $10AHPG_{10\text{-}6}$ and $20AHPG_{10\text{-}6}$) was carried out under the conditions of osteoclastic bone resorption, i.e. at a pH of about 4.5 in order to simulate the general remodelling of the skeletal system (20). Samples were immersed into water (100 ml each) at pH 4.5 and temperature 37 °C. The pH was checked and adjusted at regular intervals (2 h). If the pH was increased due to neutralization of the basic calcium phosphate, 0.001 N HNO_3 was added in order to maintain an average pH of 4.5. The samples were taken out after 72 h and weighed after being dried. The biodegradation was monitored as the change in sample weight over time. Weight loss was calculated by comparing the initial weight (W_0) with the mass measured at a given time point (W_2), as shown in Equation 2. Three individual experiments were performed, and then the average value was gained:

$$\text{Weight loss} = \frac{W2-Wo}{Wo}x100 \qquad (3)$$

3.4.3- Bioactivity testing

Standard in vitro bioactivity test was carried out to evaluate the formation of an apatite layer onto the surface of the samples. In order to study the bioactivity, the samples were soaked in simulated body fluid (SBF) which was proposed by Kokubo et al. [21] at 37 ºC and pH 7.4 for several periods of times (1, 2, 4 and 8 days**).** The specimens were removed from the SBF solution and were abundantly rinsed with water in order to remove the soluble inorganic salts and to stop the reaction.The formation and elemental composition of the bioactive layer were characterized using Philips XL 30 Scanning Electron Microscope (SEM) with an acceleration

voltage of 30 kV coupled with energy dispersive X-ray analysis (EDXA) detector with an accelerating voltage of 20 kV.

4. Results

4.1.Morphological observations

The extracted gels were dried via liquid desiccant method. The result indicating that there was a great improvement in the shrinkage values with the chemical cross-linking of alginate with Ca^{2+} ions (Figure 1). As experimentally found the alginate gels attained a level of 62% and 51% for 5 and $10AHPG_{10\text{-}6}$ gels, respectively, much more than $20AHPG_{10\text{-}6}$ one, which shrunk by an amount of 38% as shown in Table (1). The density and porosity of the obtained scaffolds are presented in the same table. Results revealed that the porosity of the alginate scaffolds varied
from 69.9% to 89.7% depending on the percentage addition of alginate. This indicates that the rigid structure of alginate formed by chemical cross-linking tends to regulate the overall pore size as well as the interconnectivity of the HA/PVA scaffolds. On the other hand, the density of the scaffold exhibited a downward trend with alginate addition. Regarding the physical property values quoted in Table (1), it goes without saying that there is a complete agreement between them. Saying in practical terms, as the shrinkage decreases the porosity and pore size substantially increase, meanwhile the density decreases greatly.

The alginate-containing scaffolds were prepared by freeze extraction method followed by chemical cross-linking in $CaCl_2$ solution, displayed different pore morphology, as judged by SEM examination. Figure (2) depicts the SEM images of alginate scaffolds taken at two different magnifications (50× and 800×). This may be due to The G-block of alginate has correspondingly high affinities for divalent calcium ions. The resultant porous structure was found to be comprised of directionally organized pores and the pore size increases with alginate addition. The pores appear to have an elongated shape. The alginate chains appear to be orderly mineralized with HA nano-particles that cover the flat area of the polymeric ribbons which are organized in a network. A further increase of alginate causes the formation of a typical egg-box structure which is the result of anisotropic growth of isomorphological molecular units [13]. It can be seen that, the alginate-containing scaffolds have tubule-like oriented pore structure, whereas their diameter, wall thickness, and structure regularity are different. With increase in alginate content, the regularity of the oriented pore structure of the scaffold was improved. For the $20AHPG_{10\text{-}6}$, the diameters of the tubule-like macropores reached 300 μm, formed well shape conjugations by regular arrayed organization, as shown in Figure (2). There was a systematic increase in the number and size of these egg-box structures with increasing the alginate contents.

4.2. Mechanical characteristics

Figure (3) presents one of the samples during the compression test, and samples shape after compression test was conducted. Some differences in failure patterns were noticed. The barrel shape resulting from friction is clear in sample 3. As for sample 1 and 2 homogenous compression is noticed, and slight compressive instability at the edges due to work-softening of material

Using engineering stress- strain relationship did not seem convenient for such highly deformable material. So load versus displacement were captured from the output acquisition system, to be interpreted into true stress- strain curve for each tested sample. The following equations were applied to obtain true stresses and strains, taking in consideration the actual dimensions of the sample at each captured result:

Compressive true stress=load × $(h_0\text{-}h)$ /vol of sample,
Compressive true strain=lnh_0 /h

Where: h_0=initial thickness, and h=instantaneous thickness during compression.
Figure (4) presents the average true stress =strain curves for investigated scaffolds.

Straightening out (re-arrangement) in material is noticed at the first non-linear zone of all the curves. The next part is the elastic portion of the curve to be used in calculating the Young's modulus of the material (Table 2). This Linear zone located between 0.02 to 0.09 strains. Non-linear plastic zone extended from 0.07 strains till end of test, indicating matrix degradation towards failure. Maximum average true stress for sample $AHP_{10\text{-}6}$ was 6 MPa, while that for sample $20AHPG_{10\text{-}6}$ was 5Mpa.

4.3- (In-Vitro Test):

4.3.1 Water-binding capacity

Figure 5 shows the water binding capacity of the AHPG scaffolds with different alginate content. It can be observed that after 1 day of immersion, compared with HA/PVA scaffold, the water content of all the alginate scaffolds increased with the introduction of alginate, which contains negatively charged carboxylic and hydroxyl groups that can form hydrogen bonds with water. A mass increase of 320% is observed for $AHP_{10\text{-}6}$ scaffolds, while for $AHPG_{10\text{-}6}$ scaffolds, this increase ranges

from 356% to 443%. In additions, the water binding ability of the scaffolds gradually increases with further increase of alginate contents due to the increase in porosity. This result agrees with the results of the porosity analysis (Table 1).

4.3.2 Biodegradation test

Figure (6) shows the relative weights of the obtained scaffolds after 72 h in osteoclastic resorption conditions (pH=4.5) [20]. It can be observed that the rate of weight loss of the scaffolds increased with alginate additions. Among the four scaffolds, it can be seen that the scaffold with a 0 wt% alginate had a lowest weight loss rate, while the scaffolds with 20% alginate had a highest rate owing to the highest porosity and also the water binding capacity.

4.3.3 Bioactivity behavior

The $AHP_{10\text{-}6}$ and $20AHPG_{10\text{-}6}$ scaffolds were subjected to the in vitro bioactivity test. The two types of scaffolds showed same biomineralization behaviors in SBF. Figure (7) shows the SEM micrographs of the porous HA/PVA composite scaffolds after 1, 2, 4 and 8 days of immersion in SBF. After 1day immersion, a lot of tiny apatite crystals deposited on the surface of the specimens, as shown in Figure 7-b. The particles formed in vitro have a near-spherical shape. Except some large particles with a diameter of about 1–2μm, reflecting the nucleation of new mineral particles. After a longer immersion (e.g. 8 days), a more compact mineral layer was found on the samples surfaces (Figure 7-d). As reported in other study [22], the Ca–P nucleus formed on the surface of biomaterials increased both in number and coalesced with an increase in immersion time and as a consequence of particle growth from the nuclei formed at different times, there was a wide size distribution. The average particle diameter, density (number of particles per unit surface area), and total apatite mass increased with incubation time. They attributed the nucleation and growth of mineral layer on the surface to the enhanced water-uptake capability of the HA induced by the presence of polymer in the nanocomposite[23].

The presence of Ca and P was confirmed by the EDX analysis of the newly formed crystals on the AHP (Figure 8). The Ca/P peak intensity ratio was 1.5, which might be indicative of the presence of a Ca-deficient apatite. This Ca–P deposition is of greater biological interest than stoichiometric HA since the Ca/P ratio in natural bone is lower than 1.67 [24].

5. Discussion

In this study, 3D porous HA/PVA/alginate scaffolds with different alginate compositions (up to 20 wt %) were prepared from the HA/PVA/alginate mixture solutions by freeze extraction and the following chemical cross-linking of alginate. The ultimate porous morphology of a scaffold, including pore size, pore shape, porosity, mechanical and biological properties was affected by alginate addition. The mixture solutions did not show any phase separation for the mixing ratios used in this study owing to their good compatibility. The freeze-extraction step before alginate cross-linking was necessary to keep the original shape of the mixture gel disk, where the freeze-extraction process induces the physical cross-linking of polymer chains by the hydrogen bonding [13]. Hydrogen bonding is thought to be the directional interaction that causes a physical cross-link to form in the gel. The latter was then chemically cross-linked in $CaCl_2$ solution to form interpenetrating networks, as demonstrated in Figure (9).

From SEM observations, it can be seen that the scaffolds dried via liquid desiccant method exhibit the interconnected macroporous network with interconnected pore diameter of 150–300 μm. Generally, for the ideal scaffolds for bone tissue regeneration, the macropore diameter and the macropore interconnections should be larger than 100 μm [25]. If the diameters of these interconnected macropores are not large enough, tissue in-growth and vascularization will not occur efficiently In Vivo and the damaged tissue cannot be fully regenerated [26]. Most of the researchers have found that the pores between 100 μm determine osteoid growth and the pores larger than 100 lm facilitate proliferation of cells, vascular in-growth, and internal mineralized bone formation. Therefore, here these $AHP_{10\text{-}6}$ and $AHPG_{10\text{-}6}$ scaffolds have suitable macroporous structure to allow cell migration, bone ingrowth and vascularization.

The difference in the processing technique, the degree of porosity and interconnectivity of the pores in the scaffolds are some of the factors which may have contributed to the variations in the mechanical properties of the scaffolds. In the present study, the decreased compressive strength values can be attributed to presence of macropores within the scaffold; it is well known that it is difficult to achieve high compressive strength for porous materials because of the negative effects of the porous structure. So it is reasonable in this case that the compressive strength and modulus decreased with the growth of scaffold's porosity.

The degradation of the prepared scaffolds at osteoclastic resorption conditions, increased with decrease in alginate content due to the increase in

obtained porosity. These in-vitro results suggested the possibility of preparing scaffolds with different degrees of solubility for the needs for different applications. The scaffold with higher alginate composition have higher water uptake. This event may be attributed to the hydrophilicity of alginate. The scaffold with more alginate composition suffered from greater weight loss because the higher water uptake causes faster degradation of the scaffold. In this context, When the HA/PVA and alginate containing composites implanted in body using as tissue scaffold, the degradation of the composite makes room for the growth of new bone and then is substituted by new bone completely. Moreover, the surface of composite is hydrophilic; this was also confirmed by the rate of water binding capacity, which can facilitate cell adhesion, proliferation and differentiation [25]. So the obtained scaffolds, used as bone substitutes, are hopeful to activate the regeneration and remodeling of bone tissue.

The formation of HA is regarded as the essential requirement for implanted materials to bond to bone in the living body. It has been widely accepted that SBF can well reproduce the in vivo surface changes of certain biomaterials. Many factors affect the nucleation and growth of Ca–P in the SBF solution. The results imply HA particles were rapidly formed on the surface of the scaffolds during SBF soaking. This may be due to the enhanced water-uptake capability (increasing of hydroxyls groups) of the composite induced by the addition of PVA and alginate. This kinetics difference of surface structural change indicating the higher bone-bonding ability of the biomimetically synthesized HA/PVA and alginate containing scaffolds that is awarded by the fast formation of bone-like apatite on their surfaces within one day.

The obtained compressive strength of $AHP_{10\text{-}6}$ (contain 70wt% HA) was 6 MPa. Whereas the alginate-containing ($20AHPG_{10\text{-}6}$) possessed a compressive strength of 5MPa Comparing the obtained results with Sinha et al. [30] who conducted a study on the fabrication of HA/PVA scaffolds for tissue engineering applications using the freeze thawing technique, though their attempts to improve the mechanical properties of the porous scaffolds by incorporating HA. The obtained results show an enhancement in the compressive strength from 2.5MPa to 21.0MPa, for samples comprising 25wt, 40wt and 50wt% HA.

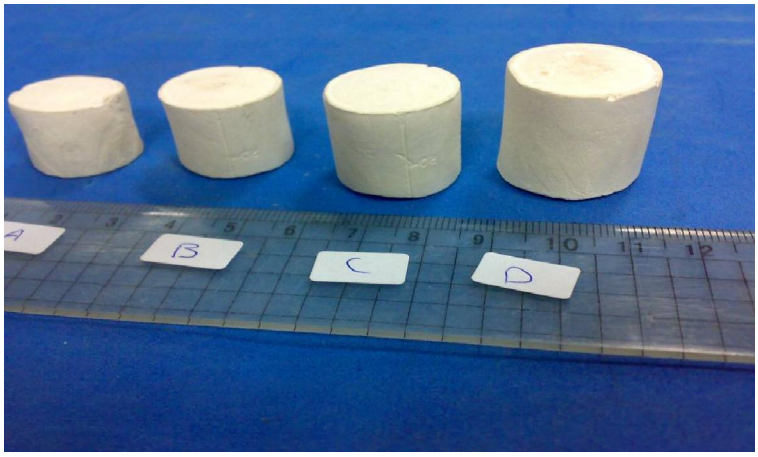

Figure (1). Photographs of scaffolds (a) AHP (b) 5AHPG (c) 10AHPG (d) 20AHPG.

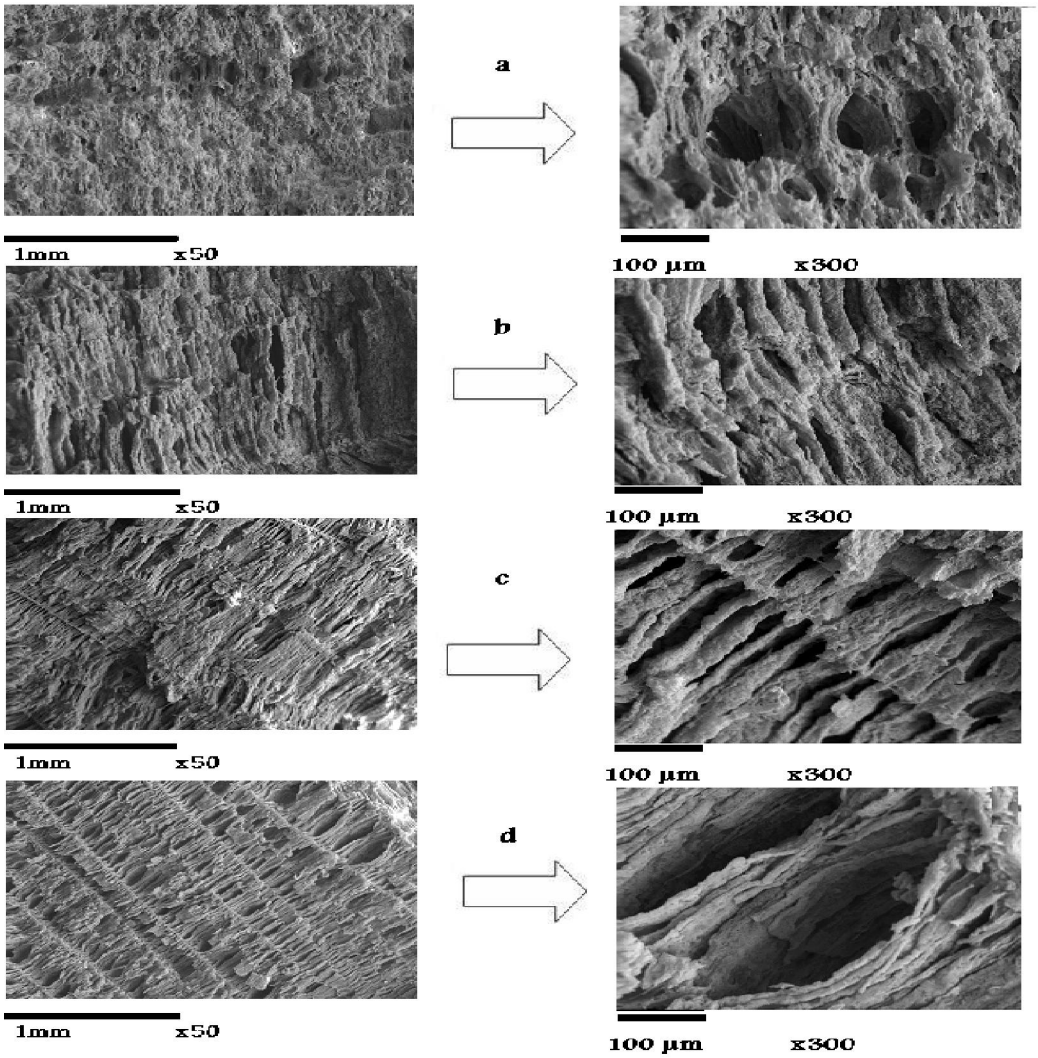

Figure (2). SEM micrographs of resultant scaffolds (a) AHP (b) 5AHPG (c) 10AHPG (d) 20AHPG.

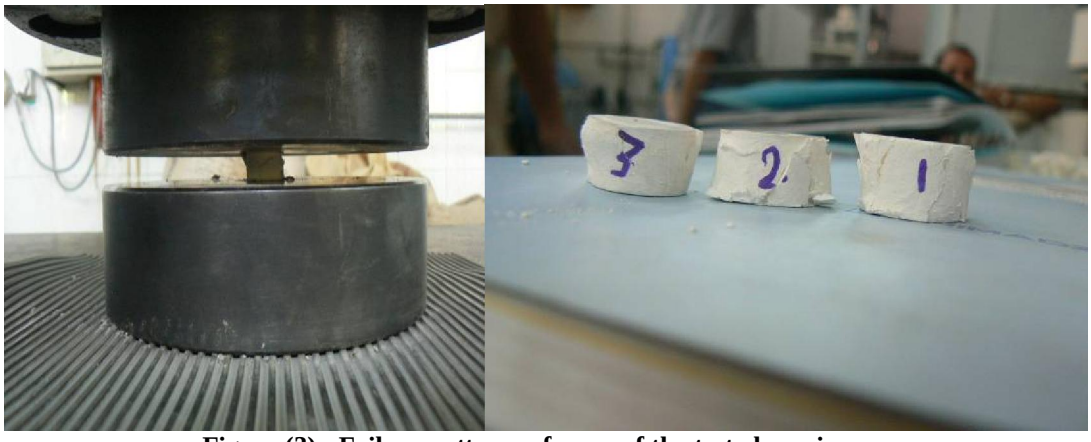

Figure (3): Failure patterns of some of the tested specimens.

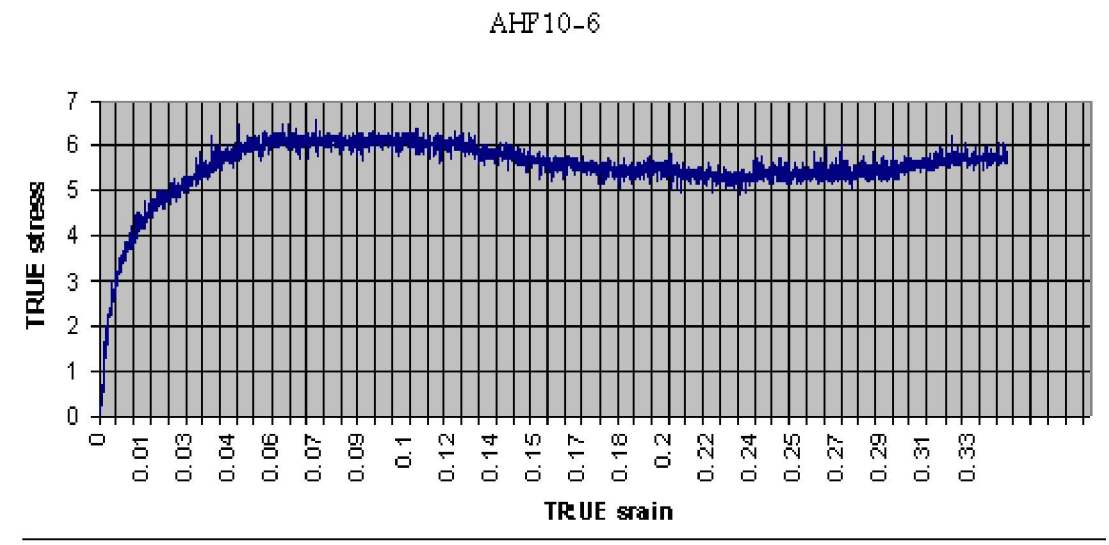

Figure (4): True stress- strain curves of tested scaffolds.

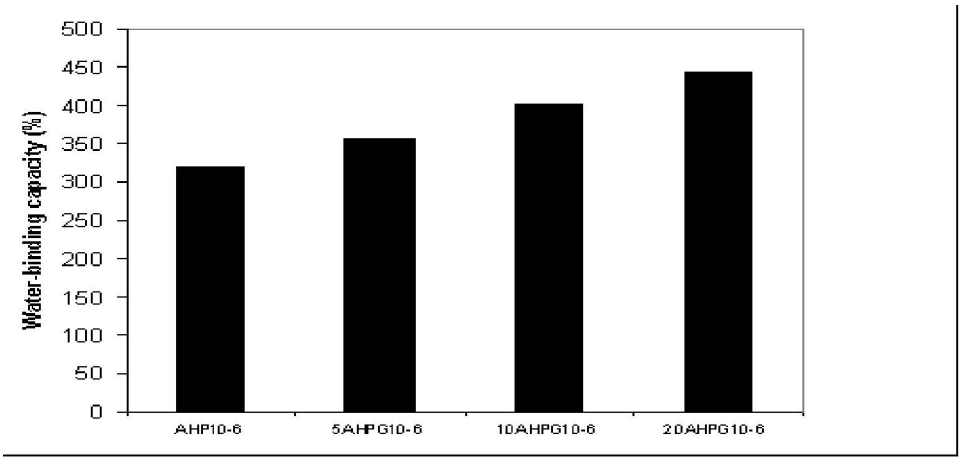

Figure (5). Water binding capacity of resultant scaffolds after one day of immersion in water.

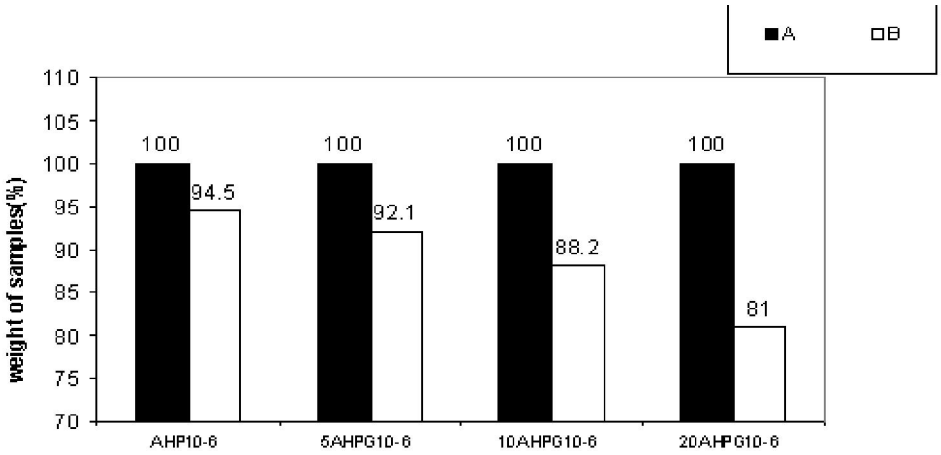

Figure (6). Biodegradation of scaffolds in water pH = 4.5 (simulation of osteoclastic resorption). A, 0 h. B,72 h.

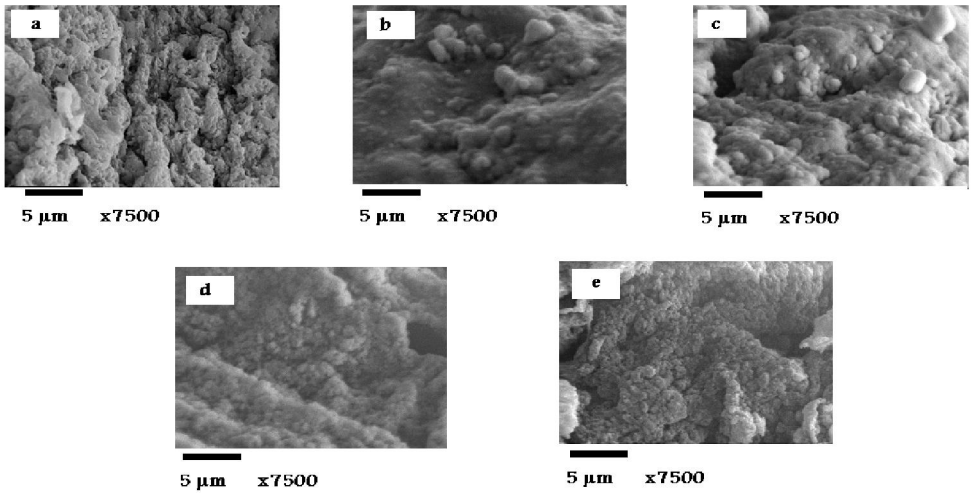

Figure (7). Morphology of the porous AHP_{10-6} scaffolds after immersion in SBF for different periods, observed by SEM: (a) 0, (b) 1, (c) 2 (d) 4 and (e) 8 days.

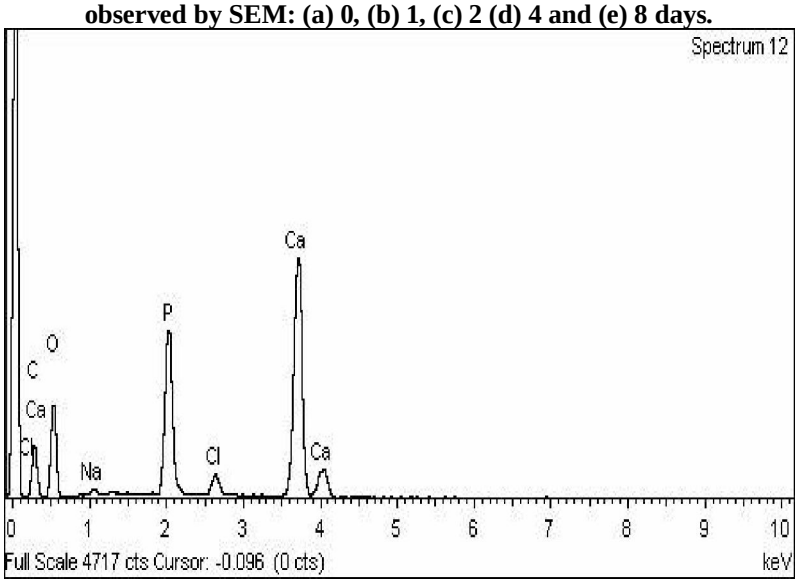

Figure (8). EDX analysis of the AHP_{10-6} scaffold after immersion in SBF for 4 days.

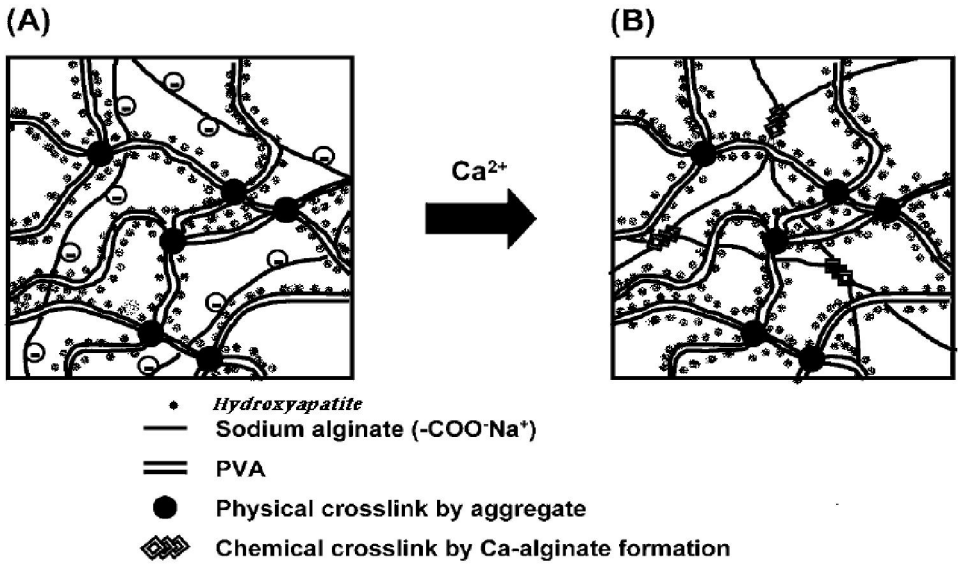

Figure (9): (a) physical cross-links of PVA chains by freeze extraction and (b) the following chemical cross-links of sodium alginate chains by $CaCl_2$.

Table (1). Density, Porosity and Related properties of the fabricated HA/PVA and alginate scaffolds.

Samples designation	Density (g/cm^3)	Porosity (%)	Maximum pore size (µm)	Degree of pores interconnectivity	Shrinkage (%)
AHP_{10-6}	0.89	62.3	150	medium	70
$5AHPG_{10-6}$	0.75	69.6	150	High	62
$10AHPG_{10-6}$	0.61	75.1	200	High	51
$20AHPG_{10-6}$	0.48	89.7	300	High	38

Table (2). Maximum compressive strength and elastic modulus of the resultant scaffolds along with cancellous bone.

Samples designation	Maximum compression strength (MPa)	Elasticity modules (MPa)
AHP_{10-6}	6	85.3
$20AHPG_{10-6}$	5	44.7
Cancellous bone	2 - 12	50 - 500

6. Conclusions

- A series of characteristic interconnected open pore microstructures with pore sizes ranging from 150 to 300 microns were fabricated by a modified freeze-extraction method including the physical cross-linking of PVA and the following chemical cross-linking of alginate.
- The porosity of the scaffolds was found to vary from 62.9% to 89.7% depending on the percentage addition of alginate. This indicates that the rigid structure of alginate formed by chemical cross-linking tends to regulate the overall pore size as well as the interconnectivity of the scaffolds. On the other hand, the density of the scaffold exhibited a downward trend with alginate addition.
- The compressive strength of spongy bone is in the range of *2–12MPa*. Hence, the measured compressive strength *(5-6 MPa)* of the present scaffolds falls in this range.
- In-vitro water binding capacity and biodegradation studies, clearly demonstrates that

it is possible to fine-tune the biodegradation and correspondingly the biological lifetime of the scaffolds by varying the alginate contents ratios. The characteristics of the resultant nanocomposite scaffolds indicating that the addition of alginate provided a more promising scaffold for tissue engineering applications.

- A biologically active apatite layer forms within a short period on composite scaffolds after its immersion in SBF, demonstrating high *in vitro* bioactivity of the composite.
- The goal of an ideal scaffold that provides good mechanical support temporarily while maintaining bioactivity and that can biodegrade at later stages at a tailorable rate is achievable with the developed alginate containing scaffolds.

7- Acknowledgement

The authors wish to thank The National Research Center of Egypt, for facilitating this fruitful co-operation between both departments, which facilitated the investigation of the proposed scaffoldings from different aspects.

8- References

[1] B.D. Ratner, S.J.Bryant., Annu Rev Biomed Eng (2004); 6:41-75.
[2] A. Atala , Exp Opin Biol Ther (2005); 5(7):879-92.
[3] J.M Pachence, J. Ln Kohn, RP Lanza, R. Langer, J. Vacanti, Principles of tissue engineering. San Diego: Academic Press; (2000).
[4] E.L.Chaikof, et al, Academic Science (2002); 961:96-105.
[5] D.W. Hutmacher, Biomaterials Jr. (2000); 21:2529–43.
[6] W. Suchanek, M. Yoshimura, J Mater Res (1998); 13:94–117.
[7] R.Z. LeGeros, P.W.Brown, B. Constantz, editors. Biological and synthetic apatites. Boca Raton: CRC Press; (1994).
[8] M. Jarcho,. Clinical Orthop Relat Res (1981); 157:259–78.
[9] T. Kitsugi, T. Yamamuro, T. Nagamura, S. Kotani, T. Kokubo, H.Takeuchi,., Biomaterials Journal (1993); 14:216–24.
[10] S. Yang, K.-F. Leong, Z. Du, C.-K. Chua, The design of scaffolds for use in tissue engineering. Part I. Traditional factors, Tissue Eng. 7 (6) (2001) 679–689.
[11] T. Yamaoka, Y. Tabata, Y. Ikada, Comparison of body distribution of poly(vinyl alcohol) with other water-soluble polymers after intravenous administration, J. Pharmaceut. Pharmacol. 47 (1995) 479–4
[12] A.P.V. Pereira, L.V. Wander, R.L. Orefice, Novel multicomponent silicate–poly(vinyl alcohol) hybrids with controlled reactivity, J. Non-Cryst. Solids 273 (2000) 180–185.
[13] S S. H. Cho et al. J. Biomater. Sci. Polymer Edn, (2005) Vol. 16, No. 8, pp. 933–947.
[14] M.G. Cascone, N. Barbani, C. Cristallini, P. Giusti, G. Ciardelli, L. Lazzeri, Bioartificial polymeric materials based on polysaccharides, J. Biomater. Sci. Polym. Edn. 12 (3) (2001) 267–281.
[15] M. Kierstan and C. Bucke, Biotechnol. Bioeng. **19**, 387 (1977).
[16] K. Nilsson, W. Scheirer, O. W. Merten, L. Ostberg, E. Liehl and H. W. D. Katinger, Nature **302**, 629 (1983).
[17] L. Shapiro and S. Cohen, Biomaterials 18, 583 (1997).
[18] E. Tolba.; B. Abd El-Hady; M. El-Tonsy, and B. El-Kholi, Egypt. J. of Appl. Sci., 24(12B) 2009.
[19] ASTM Designation: (2000). C 20-92.
[20] N. Rameshbabu, K.P. Rao., Current Applied Physics 9 (2009) S29–S31
[21] T. Kokubo., H.Kim., M. Kawashita, H. Takadama.,T. Miyazaki, M. Uchida,. And T. Nakamure, Glastech. Ber. Glass Sci. Tech. (2001); 73: 247-254.
[22] I.B.Lonor, A. Ito, K.Onuma, Kanzaki N, R.L.Reis,Biomaterials 2003; 24:579–85.
[23] D.Z. Chen et al, .Composites Science and Technology 67 (2007) 1617–1626.
[24] T. Kobayashi, S. Nakamura, K. Yamashita, J Biomed Mater Res 2001; 57:477–84.
[25] K. J. Burg, S. Porter, J. F. Kellam, Biomaterials 2000, 21, 2347.
[26] S.F. Hulbert, F.A. Young, R.S. Mathews, J.J. Klawitter, C.D. Talbert, F.H. Stelling, Potential ceramic materials as permanently implantable skeletal prostheses, J. Biomed. Mater. Res. 4 (3) (1970) 433–456.
[27] S. Rammelt, T. Illert, S. Bierbaum, Biomaterials 27 (2006) 5561.
[28] J. Zhao et al, . Colloids and Surfaces B: Biointerfaces 74 (2009) 159–166.
[29] QI. Xiaopeng, YE. Jiandong,W. Yingjun,. JR. Biomed Mater Res (2009) 89A: 980–987.
[30] A. Sinha et al, Materials Science and Engineering C. (2007), 27, 70–74.